Available online at www.sciencedirect.com
SCIENCE DIRECT®
Pergamon
Ocean Engineering 30 (2003) 1387–1415
OCEAN ENGINEERING
www.elsevier.com/locate/oceaneng

System identification of distributed-parameter marine riser models

J.M. Niedzwecki *, P.-Y.F. Liagre [1]

Department of Civil Engineering, Texas A&M University, College Station, Texas, USA

Received 17 April 2002; accepted 24 July 2002

Abstract

Modeling engineering problems of interest often requires some type of discretization model of the physical system and quite naturally leads to a mathematical description involving partial differential equations whose coefficients are dependent on both time and spatial location. In this study a reverse system identification approach is presented that utilizes generalized coordinate and force functions to recover the value of the key system parameters for each mode of vibration. To illustrate the analysis procedures, a single marine riser with general damping-restoring types of non-linearities subject to random wave excitation is considered. Analytical expressions as functions of the modes for bending stiffness and tension are derived and used for comparison with the results obtained using system identification. Numerical simulations including band-limited white noise and random wave excitation are used to explore the adequacy of the methodology and the benefits of using modal analysis in the system identification procedure. Finally, the use of and comparison with experimental data is presented and the frequency variation of parameters obtained resulting from system identification procedures discussed. Collectively, the examples demonstrate that this system identification methodology accurately identifies system parameters over portions of the frequency range of interest.

1. Introduction

Many engineering problems are best modeled as distributed-parameter systems. The governing equations describing the dynamic behavior of these systems require derivatives of the response with respect to two or more independent variables usually

* Corresponding author. Tel.: 001-979-845-2438; fax: 001-979-845-6156.
[1] Submitted for review to the Journal of Ocean Engineering April 16, 2002.

0029-8018/03/$ - see front matter © 2003 Elsevier Science Ltd. All rights reserved.
doi:10.1016/S0029-8018(02)00110-5

time and position or angle. Mathematically describing their behavior leads to either a single partial differential equation or to a coupled system of partial differential equations with constant coefficients. The objective of system identification is evaluation of the key problem parameters from time series data, based upon the form of the governing equation or equations. Linear and nonlinear system identification is an extensively developed subject where very efficient methods combining time and frequency domain methods have been developed to extract information about key system parameters from measured records of excitation and response data (see for example Imai et al., 1989; Bendat, 1990; Rice and Fitzpatrick, 1991; Bendat, 1998).

A reverse dynamic nonlinear systems identification technique for multiple-input/single-output (MI/SO) problems described by means of ordinary differential equations was presented by Bendat (1990, 1993, 1998). The power of the remarkable reverse MI/SO technique is that a nonlinear system model with feedback can be transformed into an equivalent reverse dynamic MI/SO linear model without feedback. The resulting system is then decomposed into a number of linear sub-systems that involve the computation of various conditioned (residual) spectral density functions that successively eliminate the linear contents between the inputs and the output. Using this procedure typical system parameters including, the mass, stiffness and damping, as well as, the coefficients associated with a general nonlinear damping-restoring term can be evaluated from the frequency domain results. Application of this approach to investigate a variety of two-degree of freedom nonlinear system can be found in the technical book by Bendat and Piersol (1992). Later Bendat and Piersol (1993) pointed out that estimation procedures based on frequency response functions for single-input/single-output (SI/SO) systems can easily be extended to arbitrary distributed-parameter systems subjected to distributed inputs if the system can be described in terms of its normal modes. In 1998 Bendat showed how to replace six degree of freedom (DOF) nonlinear models for ocean engineering applications with equivalent reverse linear models that can be solved by the linear data analysis procedures.

The parameters of physical systems and engineering problems of interest are generally distributed in space, and thus system identification methods must be extended to deal with distributed-parameter systems. Banks and Kunisch (1989) published a monograph, which summarized their development efforts on parameter identification analyses of distributed-parameter systems. The monograph focus is on approximation methods for least squares inverse problems governed by partial differential equations and addresses issues of the identifiably and stability of the estimated parameters. Specific results dealing with the approximation and estimation of coefficients in linear elliptic equations were presented and discussed.

Some previous studies have addressed aspects that are connected with the approach taken in this study of marine riser dynamics. Stansby et al. (1992) investigated different forms of the extended Morison equation including extra terms such as Duffing type force. The inclusion of the extra terms in the force was used to address specific consideration of vortices rather than the more general view of non-linearities taken in this present study. Jones et al. (1995) indicated that standard decay tests for the evaluation of the damping are not readily available for large structures and that the

only economical approach is to use ambient vibration data. Based upon similar logic, it seems reasonable that the system identification approach presented herein addresses the use of field or laboratory excitation of marine risers by ocean wave and currents. A compliant single degree of freedom system was studied by Panneer-Selvam and Bhattacharyya (2001). They considered four different data combination scenarios and developed an iterative scheme for the identification of the hydrodynamic coefficients in a Morison type excitation model and included in their analysis a non-linear stiffness parameter (Duffing coefficient). Their analysis procedure used reverse MI/SO technique and their findings showed that the approach was robust for both weak and strongly nonlinear systems.

In this study, a production riser for a deepwater structure is considered and Bendat's MI/SO reverse identification technique is extended to address distributed-parameter multi-DOF systems that include general nonlinear damping-restoring terms. It is assumed that the physical properties of the marine riser, e.g. mass, stiffness, etc., are constant along the length of the riser. Thus, the resulting coupled partial differential equations involve two independent variables, time and location along the axis. The discretization of the marine riser is carried out with the objective of accurately modeling the excitation and obtaining accurate modal responses to compare with data that measured displacement at a single elevation in the laboratory tests. The analysis illustrates the use of modal analysis and the nature of the convergence of modal parameter estimates for random ocean wave excitation of the marine riser.

2. Mathematical model

2.1. Derivation of the governing equation

The partial differential equation for the riser motion can be developed from first principles. Because of the symmetry of the marine riser cross-section, the equations of motions in the two principal vertical planes are identical and can be derived independently for each plane. The coupling in the direction of the wave excitation originates from relative motion between the response and the excitation. The resulting non-linear hydrodynamic drag forces are calculated using the modified Morison equation with a correction for the variation in free surface elevation as the waves pass the marine riser. As shown on Fig. 1, the length of the differential element is dx. At both end of the segment, the internal member forces are shown, and these include the shear, V, the moment, M, and axial forces, T_e. The resultant of all the external loads $f(x,t)$ and inertia forces $f_I(x,t)$ are shown at the midpoint of the segment.

Summing the forces acting on the differential element in the horizontal plane yields

$$\frac{\partial V(x,t)}{\partial x} = f(x,t) - f_I(x,t) - f_D(x,t), \tag{1}$$

where, $f_D(x,t)$ represents the medium (air or water) resistance associated with the

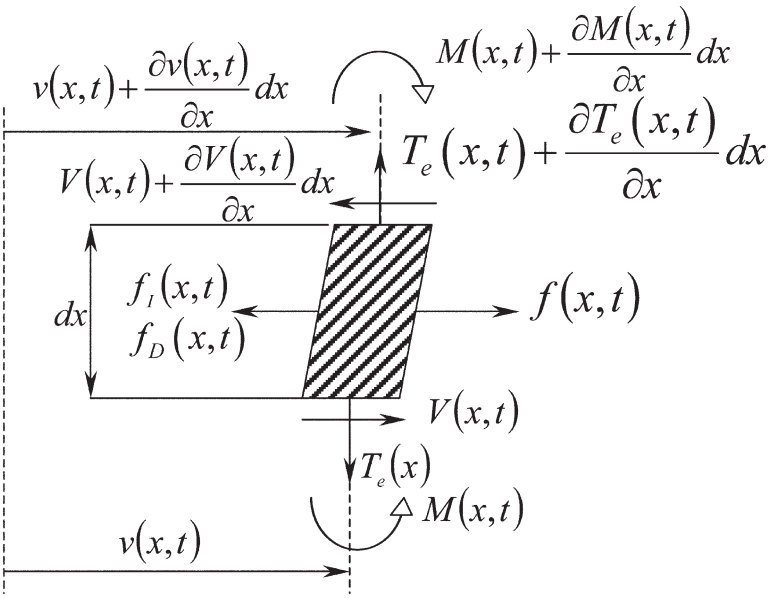

Fig. 1. Forces acting on differential marine riser element.

linear viscous damping parameter $c(x,t)$ and $f_I(x,t)$ represents the transverse inertial force given as the first derivative of the linear momentum with respect to time, specifically

$$f_I(x,t) = \frac{\partial}{\partial t}\left(m(x,t)\frac{\partial v(x,t)}{\partial t}\right). \tag{2}$$

Here the mass per unit length, $m(x,t)$, represents the sum of the marine riser structural mass and that its internal fluid mass, and, $v(x,t)$, is the horizontal displacement of the marine riser. Assuming that the mass is constant over each differential element and substituting this result into Eq. (1) yields the following expression

$$\frac{\partial V(x,t)}{\partial x} = f(x,t) - m(x)\frac{\partial^2 v(x,t)}{\partial t^2} - c(x,t)\frac{\partial v(x,t)}{\partial t} \tag{3}$$

The moment-equilibrium can be expressed as

$$V(x,t)dx = -T_e(x,t)\frac{\partial v(x,t)}{\partial x}dx + \frac{\partial M(x,t)}{\partial x}dx \tag{4}$$

Introducing this result into Eq. (3) and recalling the basic moment-curvature relationship for constant bending stiffness, EI,

$$M(x,t) = EI\frac{\partial^2 v(x,t)}{\partial x^2} \tag{5}$$

one obtains

$$EI\frac{\partial^4 v(x,t)}{\partial x^4} - T_e(x,t)\frac{\partial^2 v(x,t)}{\partial x^2} - \frac{\partial T_e(x,t)}{\partial x}\frac{\partial v(x,t)}{\partial x} + m(x)\frac{\partial^2 v(x,t)}{\partial t^2} + c(x,t)\frac{\partial v(x,t)}{\partial t} = f(x,t) \tag{6}$$

As described in McIver and Olson (1981), for most purposes the axial tension can be computed from the weight per unit length w, assuming that the riser remains nearly vertical. Each segment of the riser is subjected to an effective tension $T_e(x,t)$ of the form

$$T_e(x,t) = T_{top} - \int_x^L w(\varepsilon,t)\,d\varepsilon \tag{7}$$

where, T_{top}, is the applied tension at the top of the riser and, w, is equal to the product of the mass per unit length and acceleration of gravity for the elements located above the free surface of the waves and the buoyant weight for totally submerged elements. In the numerical simulations this problem variable is allowed to vary with position and time in order to address the undulation of the wave free surface in the wave zone.

Finally, substituting Eq. (7) into Eq. (6) yields

$$EI\frac{\partial^4 v(x,t)}{\partial x^4} - T_e(x,t)\frac{\partial^2 v(x,t)}{\partial x^2} - w(x,t)\frac{\partial v(x,t)}{\partial x} + m(x)\frac{\partial^2 v(x,t)}{\partial t^2} + c(x,t)\frac{\partial v(x,t)}{\partial t} = f(x,t) \tag{8}$$

This quasi-linear fourth order partial differential equation governs the riser response to a general dynamic and distributed external excitation $f(x,t)$. Discretization of the mariner riser along the spatial coordinate, x, leads to the development of a coupled system of governing equations.

2.2. Wave force excitation: classical approach

The primary environmental loading addressed in this study is due to ocean surface waves, although it is straightforward to consider ocean currents as well. Because a marine riser is basically a slender body, the in-line wave force can be computed using the well-known Morison equation that is the sum of the drag and inertia force components. Also it is assumed that in the sub-sea region near the marine riser, the kinematics of the flow do not change in the incident wave direction. Taking into account the relative motion between the marine riser and the flow-induced kinematics, the drag force per unit length can be expressed as

$$f_D(x,t) = C_D(R_e(x,t))\ \frac{\rho_w D}{2}\left(u(x,t) - \frac{\partial v(x,t)}{\partial t}\right)\left|u(x,t) - \frac{\partial v(x,t)}{\partial t}\right| \tag{9}$$

where, $u(x,t)$ is taken as the horizontal component of the water particle velocity,

D is the outer marine riser diameter, ρ_w, the water density and, C_D, the drag coefficient function which is a function of the local Reynolds number $R_e(x,t)$. Correspondingly, the inertia force per unit length is of the form

$$f_M(x,t) = C_M \frac{\rho_w \pi D^2}{4} \frac{\partial u(x,t)}{\partial t} - C_A \frac{\rho_w \pi D^2}{4} \frac{\partial^2 v(x,t)}{\partial t^2} \tag{10}$$

where, C_M is the inertia coefficient, herein assumed to be constant. The relationship between the inertia coefficient and the hydrodynamic added-mass coefficient is given as, $C_M \equiv C_A + 1$.

Moving the hydrodynamic added-mass, to the left side of governing equation yields

$$EI\frac{\partial^4 v(x,t)}{\partial x^4} - T_e(x,t)\frac{\partial^2 v(x,t)}{\partial x^2} - w(x,t)\frac{\partial v(x,t)}{\partial x} + M(x)\frac{\partial^2 v(x,t)}{\partial t^2} + c(x,t)\frac{\partial v(x,t)}{\partial t} = f(x,t) \tag{11}$$

where,

$$M(x) = m(x) + C_A \frac{\rho_w \pi D^2}{4} \tag{12}$$

and the wave force excitation, $f(x,t)$, per unit length is then

$$f(x,t) = C_M \frac{\rho_w \pi D^2 \partial u(x,t)}{4 \partial t} + C_D(R_e(x,t)) \frac{\rho_w D}{2}\left(u(x,t) - \frac{\partial v(x,t)}{\partial t}\right)\left|u(x,t) - \frac{\partial v(x,t)}{\partial t}\right| \tag{13}$$

The last term in this equation represents the nonlinear drag force due to the relative motion between the fluid and the structural response, and it acts effectively to reduce, i.e. dampen, the motion response of the marine riser. Often in practice the nonlinear drag force is linearized resulting in the separation of the kinematic contributions. For example, Sarpkaya and Isaacson (1981) consider an approach where the quadratic term of the drag force due to the relative fluid velocity is replaced by a linear expression involving the root mean square value of the relative velocity, $\sigma_{\dot{r}}$. Then introducing this approximation and combining Eqs. (11) and (13) one obtains

$$EI\frac{\partial^4 v(x,t)}{\partial x^4} - T_e(x,t)\frac{\partial^2 v(x,t)}{\partial x^2} - w(x,t)\frac{\partial v(x,t)}{\partial x} + M(x)\frac{\partial^2 v(x,t)}{\partial t^2} + \left[c(x,t) + C_D \frac{\rho_w D}{2}\sqrt{\frac{8}{\pi}}\sigma_{\dot{r}}\right]\frac{\partial v(x,t)}{\partial t} = f_L(x,t), \tag{14}$$

with the applied loading of the form

$$f_L(x,t) = C_M \frac{\rho_w \pi D^2 \partial u(x,t)}{4 \quad \partial t} + C_D \frac{\rho_w D}{2} \sqrt{\frac{8}{\pi}} \sigma_{\dot{r}} \; u(x,t). \tag{15}$$

Often as a first approximation, the wave damping due to the relative motion can be simplified assuming that $\sigma_{\dot{r}} \simeq \sigma_u$. Other approximations are available in the open literature such as that proposed by Krolikowsky and Gay (1980) for dealing with waves and currents.

2.3. Wave force excitation: non-classical approach

As one begins to think about the range of sources for non-linear behavior that are possible, other approaches to modeling the non-linear response behavior need to be considered. In this study, it is suggested that the nonlinear drag force be treated more generally following the approach suggested in nonlinear system identification where,

$$EI\frac{\partial^4 v(x,t)}{\partial x^4} - T_e(x,t)\frac{\partial^2 v(x,t)}{\partial x^2} - w(x,t)\frac{\partial v(x,t)}{\partial x} + M(x)\frac{\partial^2 v(x,t)}{\partial t^2} + c(x,t)\frac{\partial v(x,t)}{\partial t} + p(x,\dot{x},\ldots,t) = f_L(x,t) \tag{16}$$

where, $p(x,\dot{x},\ldots,t)$ can take on classical forms such as the Duffing, Van der Pol or polynomial types of non-linearities. In this study a general non-linear damping-restoring term based upon the combination of classic Duffing and Van der Pol nonlinearities is used, specifically,

$$p(x,\dot{x},...,t) = k_3 \; v^3(x,t) + \frac{c_3}{3}\frac{\partial v^3(x,t)}{\partial t}, \tag{17}$$

where, k_3, is the Duffing coefficient and, c_3, is the Van der Pol coefficient. The Duffing non-linearity acts as an artificial spring with variable positive stiffness, $k_3(x)\; v^2(x,t)$, that increases as the displacement, $v(x,t)$, gets larger. Such a spring grows stiffer as the riser differential elements moves away from its equilibrium position, but it recovers its original value when the segments return to their original position. Thus, high-amplitude excursions should oscillate faster than low-amplitude ones, and the sinusoidal shapes should be "pinched in" at their peaks. The Van der Pol non-linearity acts as an additional damper. The nature of Eq. (17) will become more evident in the derivation of the system identification approach.

2.4. Modeling the wave kinematics

Linear wave theory is adopted as the basis for modeling regular and random wave trains used in this study. It should be noted that the system identification approach to be presented in the next section is not limited by this assumption, and any wave theory of choice can be utilized. Here the wave kinematics are modified using Wheeler stretching technique (Wheeler, 1970) to obtain the wave kinematics up to

the actual free surface. It is assumed that the wave scattering due to the wave-riser interaction is negligible.

A standard random phase approach is taken to describe a uni-directional random seaway, in particular the random sea surface elevation is assumed of the form

$$\eta(t) = \sum_{j=1}^{\infty} A_j \cos(\omega_j t + \phi_j), \tag{18}$$

where, A_j, is the wave component amplitude obtained based upon a particular random sea model, ω_j is the corresponding wave frequency and ϕ_j is the random phase angle assumed to be uniformly distributed over the interval $[0,2\pi]$. Consistent with linear wave theory, the horizontal water particle velocity and acceleration are expressed respectively as

$$u(x,t) = \sum_{j=1}^{\infty} A_j \omega_j \frac{\cosh(k_j x)}{\sinh(k_j d)} \cos(\omega_j t + \phi_j) \tag{19}$$

$$\frac{\partial u(x,t)}{\partial t} = \sum_{j=1}^{\infty} A_j \omega_j^2 \frac{\cosh(k_j x)}{\sinh(k_j d)} \sin(\omega_j t + \phi_j) \tag{20}$$

where, k_j is the wave number and is related to ω_j through the linear dispersion relation for a specified water depth d, as

$$\omega_j^2 = g k_j \tanh(k_j d). \tag{21}$$

A snapshot of the horizontal wave kinematics, velocity and acceleration, computed from the wave elevation recorded during a uni-directional random wave test is presented in Fig. 2.

3. System identification

System identification procedures for non-linear systems with feedback can be can be computationally laborious and the procedures can have difficulty in distinguishing between linear and non-linear contributions. Bendat (1990) developed an interesting alternative procedure for nonlinear system identification. In his procedure, the roles of the physical input $f(x,t)$ and physical output $v(x,t)$ are first to be inverted to create a reverse dynamic nonlinear model with no feedback. For this study, an equivalent reverse dynamic two-input/single-output linear model is presented and is based upon the mathematical marine partial differential equations previously discussed.

3.1. Two-input/single-output reverse dynamic linear model

Consider the partial differential Eq. (16) that governs the riser response for any given applied force $f(x,t)$. The physical properties as well as the tension are assumed

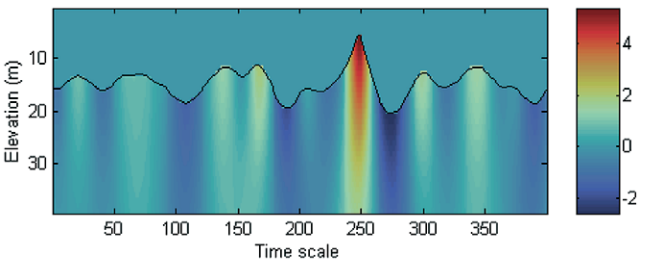

(a)

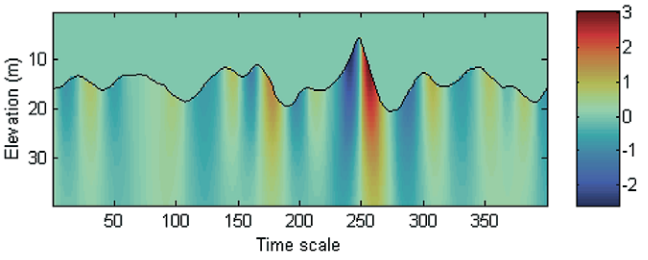

(b)

Fig. 2. Contours of random wave kinematics: (a) horizontal component of wave velocity and, (b) corresponding horizontal acceleration.

to be uniform along the length of the riser and not to vary with time, thus one obtains a further simplified model of the marine riser governed by the expression

$$EI\frac{\partial^4 v(x,t)}{\partial x^4} - T\frac{\partial^2 v(x,t)}{\partial x^2} + m\frac{\partial^2 v(x,t)}{\partial t^2} + c\frac{\partial v(x,t)}{\partial t} + k_3 v^3(x,t) + \frac{c_3}{3}\frac{\partial v^3(x,t)}{\partial t} = f(x,t) \tag{22}$$

The non-linearity of the dynamic system, caused by the interaction of fluid and structural kinematics, is included in $f(x,t)$, which is selected as a base function (Narayanan and Yim, 2000).

Solving the eigenvalue problem for natural frequencies and mode shapes, see for example Clough and Penzien (1993), the dynamic response of the riser at any location x and time t is given by a linear combination N modes, specifically

$$v(x,t) \simeq \sum_{i=1}^{N} \phi_i(x) P_i(t), \tag{23}$$

where, $\phi_i(x)$ and $P_i(t)$ are the usual mode shape and generalized coordinate for the i^{th} normal mode. Similarly it is assumed that the cubic term can be expanded in terms of the same mode shapes, $\phi_i(x)$, and the new generalized coordinate $Q_i(t)$ of the i^{th} normal mode

$$v^3(x,t) \cong \sum_{i=1}^{N} \phi_i(x) Q_i(t). \tag{24}$$

Introducing Eqs. (23) and (24) into Eq. (22) leads to the following expression

$$\sum_{i=1}^{N} m\,\phi_i(x)\ddot{P}_i(t) + \sum_{i=1}^{N} c\,\phi_i(x)\,\dot{P}_i(t) + \sum_{i=1}^{N} (EI\phi_i^{iv}(x) - T\phi''_i(x))P_i(t) + \sum_{i=1}^{N} k_3\,\phi_i(x)\,Q_i(t) + \sum_{i=1}^{N} \frac{c_3}{3}\phi_i(x)\,\dot{Q}_i(t) = f(x,t) \tag{25}$$

where, the primes denote space derivatives and the overdots indicate time derivatives.

Multiplying each term by $\phi_n(x)$, integrating over the length of the riser and interchanging the order of integration and summation yields

$$\sum_{i=1}^{N} \ddot{P}_i(t)\int_0^L m\,\phi_i(x)\phi_n(x)dx + \sum_{i=1}^{N} \dot{P}_i(t)\int_0^L c\,\phi_i(x)\phi_n(x)dx + \sum_{i=1}^{N} P_i(t)\int_0^L (EI\phi_i^{iv}(x) - T\phi''_i(x))\phi_n(x)dx + \sum_{i=1}^{N} Q_i(t)\int_0^L k_3\,\phi_i(x)\phi_n(x)\,dx + \sum_{i=1}^{N} \dot{Q}_i(t)\int_0^L \frac{c_3}{3}\phi_i(x)\phi_n(x)\,dx = \int_0^L f(x,t)\phi_n(x)\,dx \tag{26}$$

By virtue of the orthogonal properties of the modes, all terms in each of the summations vanish except the one term for which $i = n$. Consequently for each mode n, Eq. (26) can be rewritten as

$$M_n\ddot{P}_n(t) + C_n\dot{P}_n(t) + K_nP_n(t) + D_nQ_n(t) + V_n\dot{Q}_n(t) = F_n(t) \tag{27}$$
$$n = 1,2,...,N$$

where, the generalized mass, damping, stiffness, nonlinear contributions and force are of the form

$$M_n = \int_0^L m\,\phi_n^2(x)dx \tag{28}$$

$$C_n = \int_0^L c\,\phi_n^2(x)\;dx \tag{29}$$

$$K_n = \int_0^L (EI\phi_n^{iv}(x) - T\phi''_n(x))\phi_n(x)dx \tag{30}$$

$$D_n = \int_0^L k_3\,\phi_n^2(x)dx \tag{31}$$

$$V_n = \int_0^L \frac{c_3}{3}\,\phi_n^2(x)\,dx \tag{32}$$

$$F_n(t) = \int_0^L f(x,t)\,\phi_n(x)dx \tag{33}$$

This set of partial differential equations constitutes the equivalent reverse dynamic two-input/single-output (TI/SO) linear model from which frequency domain relations can be derived.

For a upon pin-pin connected beam or string, the vibration shape of the n^{th} mode can be expressed as (Clough and Penzien, 1993)

$$\phi_n(x) = \sin\left(\frac{n\pi x}{L}\right) \tag{34}$$

where, L, represents the length of the marine riser. Substituting this result into Eq. (28) through (32) one obtains

$$M_n = \frac{mL}{2} \tag{35}$$

$$C_n = \frac{cL}{2} \tag{36}$$

$$K_n = \frac{EIL}{2}\left(\frac{n\pi}{L}\right)^4 + \frac{TL}{2}\left(\frac{n\pi}{L}\right)^2 \qquad n = 1,2,3,... \tag{37}$$

$$D_n = \frac{k_3 L}{2} \tag{38}$$

$$V_n = \frac{c_3 L}{6} \tag{39}$$

Finally, since the dynamic response, $v(x,t)$, is known, the generalized coordinates $P_n(t)$ and $Q_n(t)$ can be evaluated

$$P_n(t) = \frac{2}{L}\int_0^L v(x,t)\sin\left(\frac{n\pi x}{L}\right)dx \tag{40}$$

$$Q_n(t) = \frac{2}{L}\int_0^L v^3(x,t)\sin\left(\frac{n\pi x}{L}\right)dx \tag{41}$$

In the reverse dynamic model, $F_n(t)$ is the mathematical output, and $P_n(t)$ and $Q_n(t)$ are the required inputs to the system. The two inputs are computed from the dynamic response of this nonlinear system, and can be non-Gaussian and correlated to some extent. From knowledge of $P_n(t)$, $Q_n(t)$ and $F_n(t)$, without restrictions on their probability or spectral properties, the TI/SO linear system can be solved using the reverse MI/SO technique to identify the two frequency response functions, from which the system parameters can be recovered. Thus, all that remains in the formulation is the development of the frequency domain equations.

3.2. Frequency domain identification

The equivalence between the SI/SO nonlinear system and reverse dynamic TI/SO linear model featuring a linear sub-system in parallel with a nonlinear sub-system has a great significance because the frequency transfer functions between inputs $P_n(t)$ and $Q_n(t)$ and output $F_n(t)$ can be identified by MI/SO linear technique (Bendat, 1990).

Taking the Fourier Transform of both sides of Eq. (27) gives the frequency domain relation

$$E_n(f)X_n(f) + F_n(f)Y_n(f) = Z(f) \tag{42}$$

where,

$$X_n(f) = \Im[P_n(t)] \tag{43}$$

$$Y_n(f) = \Im[Q_n(t)] \tag{44}$$

$$Z_n(f) = \Im[F_n(t)] \tag{45}$$

and, $\Im[]$ indicates a Fourier transform.

Based on the computation of these three quantities, it is straightforward to compute the two frequency response functions $E_n(f)$ and $F_n(f)$

$$E_n(f) = K_n - (2\pi f)^2 M_n + j(2\pi f)C_n \tag{46}$$

$$F_n(f) = D_n + j(2\pi f)V_n \tag{47}$$

The generalized stiffness, mass and damping for the n^{th} mode of vibration are given by

$$K_n = \lim_{f\to 0} \mathrm{Re}(E_n(f)) \tag{48}$$

$$M_n = \frac{K_n - \mathrm{Re}(E_n(f))}{(2\pi f)^2} \tag{49}$$

$$C_n = \frac{\mathrm{Im}(E_n(f))}{2\pi f} \tag{50}$$

$$D_n = \mathrm{Re}(F_n(f)) \tag{51}$$

$$V_n = \frac{\mathrm{Im}(F_n(f))}{2\pi f}. \tag{52}$$

Recalling Eqs. (35), (36), (38) and (39), the mass, damping, Duffing and Van der Pol terms can be computed from any mode of vibration

$$m = \frac{2}{L}M_n \qquad \forall n = 1,2,3,... \tag{53}$$

$$c = \frac{2}{L}C_n \qquad \forall n = 1,2,3,... \tag{54}$$

$$k_3 = \frac{2}{L}D_n \qquad \forall n = 1,2,3,... \tag{55}$$

$$c_3 = \frac{6}{L}V_n \qquad \forall n = 1,2,3,.... \tag{56}$$

On the other hand, the determination and partition of the flexural stiffness and tension require the value of the generalized stiffness for at least two different modes of vibration. Knowing the generalized stiffness for two different modes of vibration p and q and recalling Eq. (37), we get a linear system with two equations and two unknowns. Solving for the tension and the flexural, or bending, stiffness are of the form

$$T = \frac{q^4K_p - p^4K_q}{\frac{L}{2}\left(q^4\left(\frac{p\pi}{L}\right)^2 - p^4\left(\frac{q\pi}{L}\right)^2\right)} \qquad \forall p \neq q \tag{57}$$

$$EI = \frac{q^2K_p - p^2K_q}{\frac{L}{2}\left(q^2\left(\frac{p\pi}{L}\right)^4 - p^2\left(\frac{q\pi}{L}\right)^4\right)} \qquad \forall p \neq q. \tag{58}$$

4. Numerical examples

A series of numerical examples is presented that explore the adequacy of the numerical implementation of the formulation to predict response behavior of a marine riser and to demonstrate the applicability of the reverse system identification technique to distributed-parameter systems. The examples utilize numerical simulations and experimental data as would be expected to be available in design practice. Emphasis is placed on motions in-line with the wave propagation and transverse vibrations, set up by vortices shedding from the cylinder, were not considered.

4.1. White noise excitation

For this example, a marine riser, 873 m long, with the properties summarized in Table 1 was studied. The marine riser was assumed to be pin-pined with the top hinge positioned 23 m above the still water level. Fig. 3 presents a characterization of the excitation that includes a time history segment of the random wave excitation, $\eta(t)$, the corresponding evidence that the process is Gaussian as demonstrated by the probability distribution, and the locally band-limited white noise spectrum used to generate the random sea surface elevation. A 5 Hz sampling frequency was selected and a lowpass Butterworth filter with a sharp cutoff at 1 Hz was applied in the generation of the white noise spectrum. The random wave elevation and linear wave theory were used to generate the wave kinematics used in the computation of the the wave loads. Since the computation of the generalized coordinates $P_n(t)$ and $Q_n(t)$ and forcing function $F_n(t)$ requires the riser motions $v(x,t)$ and force $f(x,t)$ to be integrated over the the length of the riser. The initial spatial discretization was 1 meter and the riser motions were computed at 8192 time steps, which is equivalent to a test duration of 27.3 minutes.

The mass per unit length for the first five modes of vibration identified using the reverse system identifiation model are presented in Fig. 4. Recall that the frequency range of interest is 0–1 Hz. This graph illustrates that the marine riser can be thought of as a low pass filter since the estimates of mass per unit length do not cover the white noise frequency range in its entirety. On the other hand, as can be observed in the figure, the specified mass (912 kg/m) can be recovered with good accuracy from the generalized mass of any mode of vibration. Moreover, it seems that higher mode tend to give a better accuracy over the whole frequency range. The estimates of the linear viscous damping coefficient for the first five modes of vibration are presented in Fig. 5. It can be observed that the value of the linear viscous damping is recovered with acceptable accuracy over the 0–0.5 Hz frequency range. In the 0.5–1 Hz frequency range, the scattering of the results is perhaps a consequence of the filtering action of this marine riser system. The estimates of the Duffing coefficient for the first five modes of vibration are shown in Fig. 6. Again it is observed that the estimates are accurate over only a portion for the frequency range of interest

Table 1
Marine riser particulars for white noise simulation

	Units	Specified value
Riser Length	m	873
Outer radius	m	0.7
Mass per unit length (Including added mass)	kg/m	912
Linear viscous drag coefficient	Ns/m	120
Duffing coefficient	N/m^3	8000
Van de Pol coefficient	Ns/m^3	5000
Tension	N	7×10^6
Bending stiffness	Nm^2	10^7

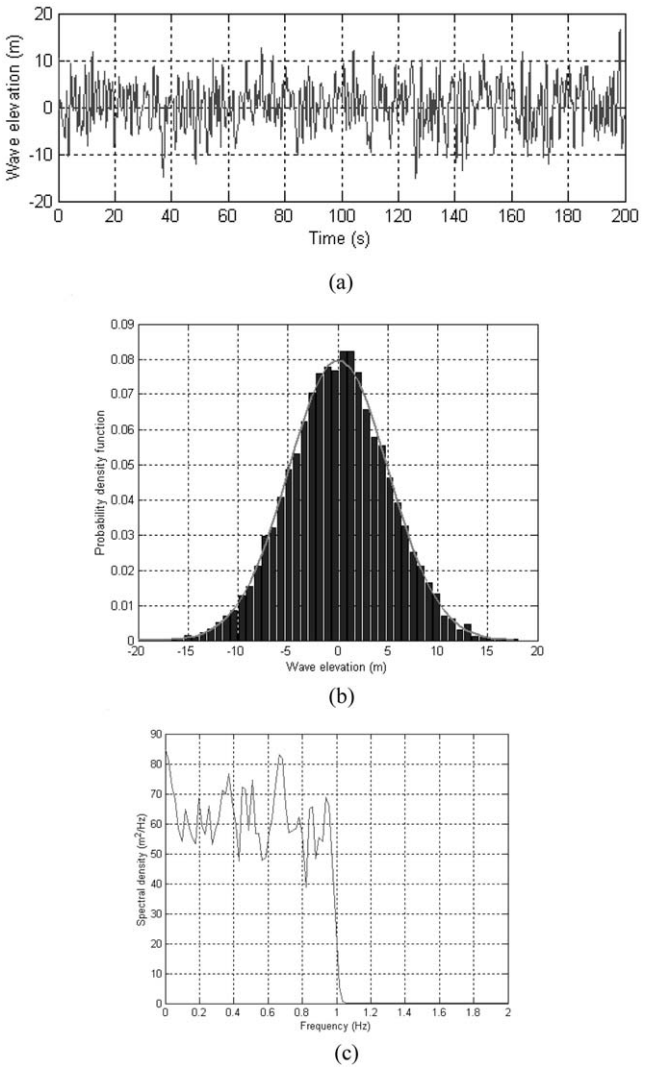

Fig. 3. Characterization of random wave excitation: (a) sample time series, (b) distribution of crest and troughs, and (c) white noise spectrum.

(0–1 Hz). This is similar to the case for the mass per unit length, and it is concluded that these results reflect the same signs of low pass filtering by the marine riser system. The estimates of the Van der Pol coefficient for the first five modes of vibration are shown in Fig. 7. This modal coefficient is less well behaved at very small frequencies. Omitting this range a reasonable estimate can be obtained for coefficient.

A comparison between the theoretical estimates for modal tension, Eq. (57), and bending stiffness variations, Eq. (58), and those recovered using the reverse system

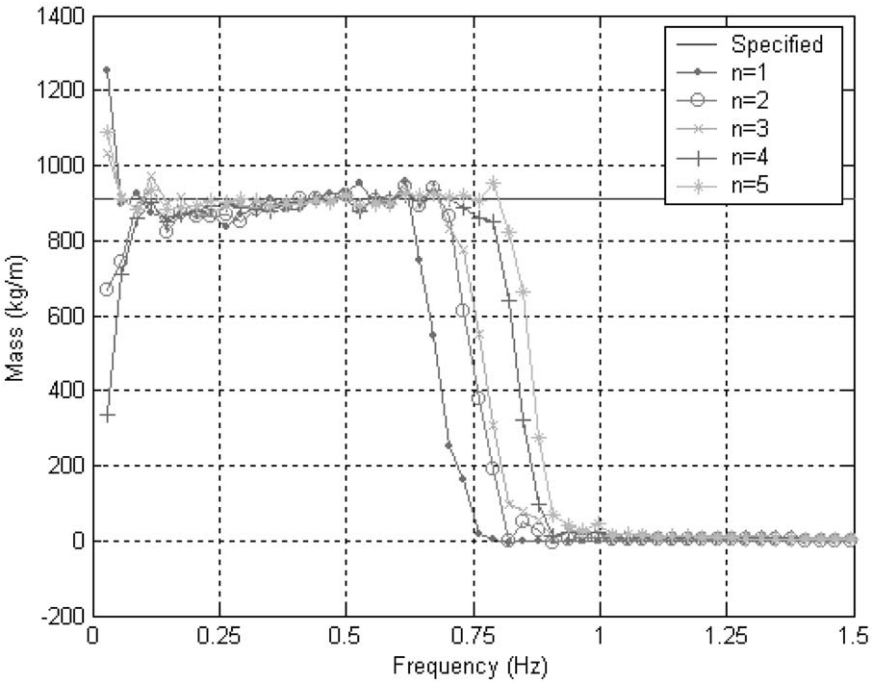

Fig. 4. Modal estimates of the mass per unit length obtained using reverse system identification.

identification method are presented in Figs. 8 and 9. The theoretical curves are well behaved, and noise free, as seen for the modes of vibration between 1 and 20. The symmetry of the figures follows the symmetry of the generalized stiffness. For both properties, the specified tension ($7 \times 10^6\,N$) and flexural stiffness ($10^7\,Nm^2$) values tend to be recovered with greater accuracy for combinations of higher modes of vibration. A summary of the system identification results are presented in Tables 2 and 3. The model estimates are quite accurate for the mass, viscous damping and Duffing coefficient. However, the Van der Pol estimates are not as good with errors ranging from six to about seventeen percent.

4.2. Comparison with model test data

A series of experiments on modeling deepwater risers and tendons was conducted in the Offshore Technology Research Center model basin (Rijken, 1997). The model test program included the consideration of pretension variations and the response to regular wave environments, as well as, multiple random sea realizations of North Atlantic design storms. The 1:55 scale riser model was constructed using an ABS casing surrounding a 2.5 mm diameter, model scale, steel rod. The steel rod carried the tension load while the snug fitting ABS sleeve created the design hydrodynamic diameter. The motion of the riser was optically tracked at approximately mid-depth,

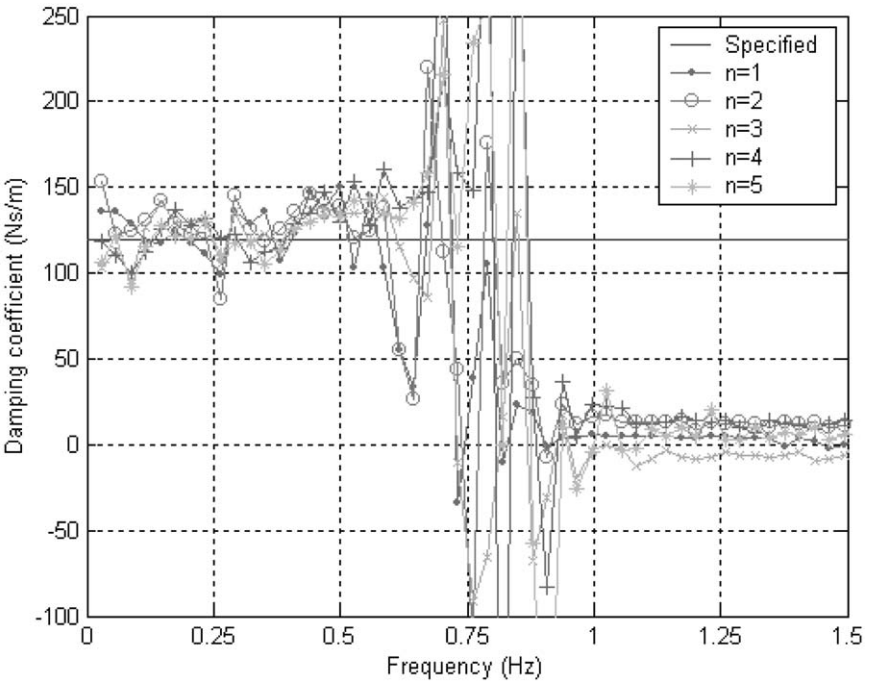

Fig. 5. Modal estimates of the viscous damping coefficient obtained using reverse system identification

5.56 m model scale or 306 m prototype scale. Four wave probes were located in a square pattern around the slender cylindrical model as shown in Fig. 10.

In model tests it is difficult to accurately match all of the prototype properties of the marine riser or tendons. With careful model building, geometric properties such as the riser external dimensions can be more easily be met. It is the mechanical properties such as moment of inertia, modulus of elasticity, etc. that can be quite difficult to match. As a result, some of the system parameters for the simulations had to be adjusted by trial and error. The particulars of the riser model are presented in Table 4.

The reverse system identification technique requires more than a single elevation measurement, because in particular, the computation of the generalized coordinates requires a number of measurements of the displacement along the riser. Thus the development of the numerical model required some careful forethought. The riser was modeled using 1-meter prototype length elements that permitted a very precise rendering of the wave forces on the riser and a clear demarcation between air and water mediums, where the force gradient is important. The mass per unit length, which includes the added mass for the submerged segments of the riser, and the effective tension were evaluated at each time step in order to account the fluctuation of the free-surface water elevation.

Fig. 11 presents a comparative look at the simulated riser in-line displacements at a depth of 306 m for the three different expressions of the governing equation,

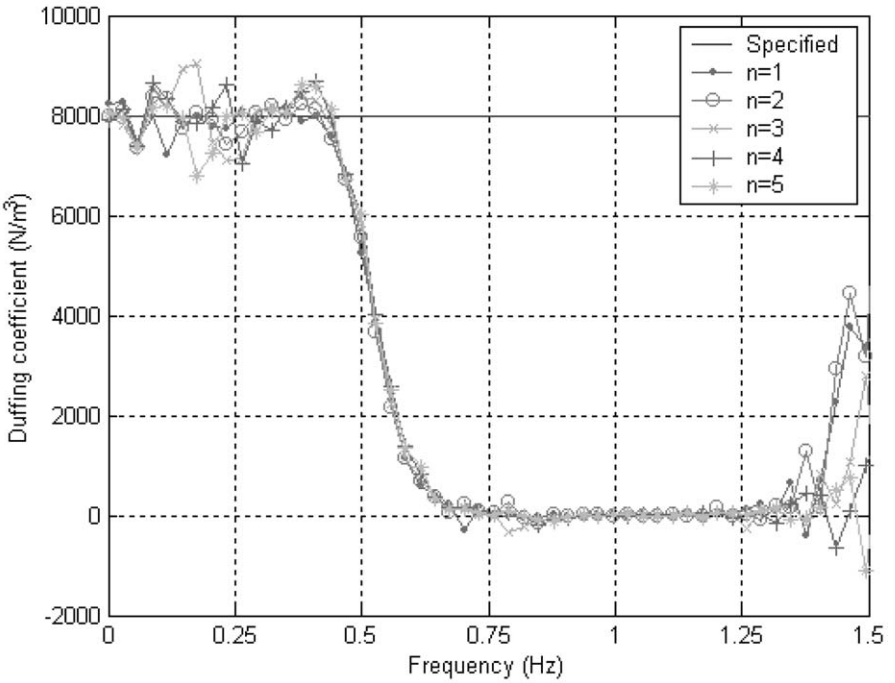

Fig. 6. Modal estimates of the Duffing coefficient obtained using reverse system identification.

specifically for the fully nonlinear model, the equivalent linear drag force model, the non-linear Duffing coefficient model, and the experimental data. The experimental signal (red solid line), over which the simulations are superimposed (blue dots), was extracted from the beginning of a random wave test. It was noticed that in some cases the experimental response exhibited chaotic behavior a few minutes into the test. This observed chaotic behavior is an outward sign of vortex-induced vibrations, which were not modeled in the present study. The simulation using the fully nonlinear governing equation shows very good agreement with the experimental data but this success was achieved at the expense of the tedious work of fine-tuning of the parameters. The agreement for the two other simulations can be described as good and easier to obtain.

The superposition of histogram and fitted normal distributions of the numerical simulations for riser displacement at 306 m are presented in Fig. 12, for the linear drag force model and the Duffing model. The effects of the Duffing coefficient model are clearly recognizable here in this figure. There are more low amplitude and fewer high amplitude oscillations than for the linear drag force simulation. This corroborates the notion that, when including the Duffing coefficient model, high amplitude excursions oscillate faster than low amplitude ones, and the sinusoidal shapes are "pinched in" at their peaks. Fine-tuning of the parameters lead to good agreement of the numerical model with the single depth measurement obtained in the laboratory testing.

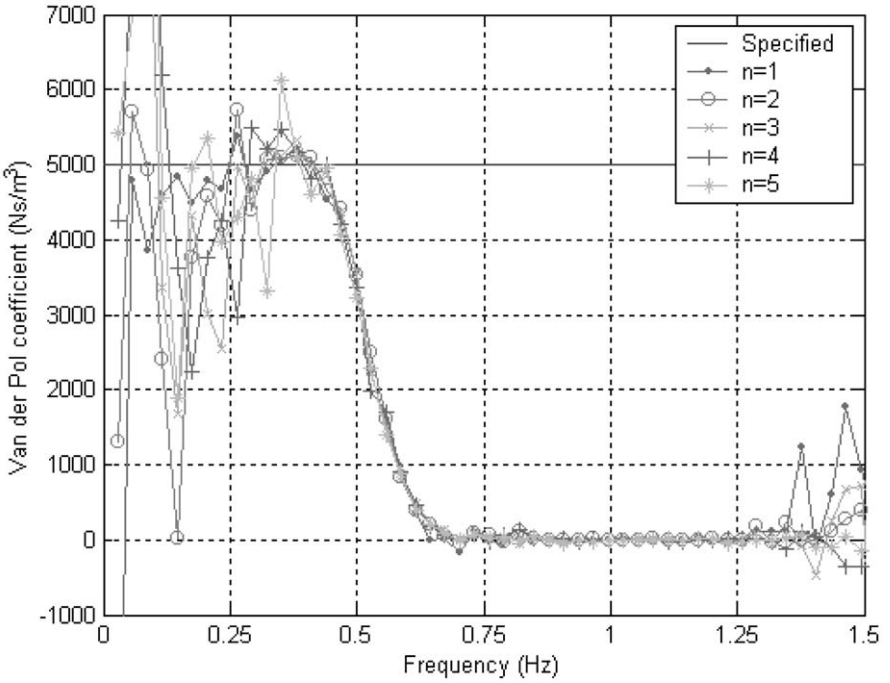

Fig. 7. Modal estimates of the Van der Pol coefficient obtained using reverse system identification.

4.3. Probabilistic interpretation of riser response behavior

To better understand the riser response behavior and the propagation of non-linear behavior due to the near surface random wave excitation, the time series response at three select elevations was systematically investigated. Before pursuing the details at specific elevations of 100, 400 and 700 m, one should consider the more global perspective presented in Fig. 13. This figure illustrates that the response envelopes and probability density functions for the various models can be quite different depending upon the type of nonlinearity that is considered appropriate. In fact, the response envelope presented in Fig. 13 (d) better resembles in a qualitative way some of the response envelopes observed in model basin tests.

The probability distributions and the corresponding statistical quantities used to characterize the distributions are presented in Fig. 14 and Table 5 respectively. It is expected that where Gaussian excitation is applied as an input to a linear system, here the linear riser model with a linear force model, the output i.e. response will also be Gaussian. The random sea excitation consisted of a wave train of 117 waves with a minimum wave elevation of -8.4375 m and a maximum wave elevation of 12.5349 m. An analysis of the wave input indicated that the design seas had a mean of 0.2741 m, a variance of 11.9205 m^2, a skewness of 0.3027 and a kurtosis of 3.0200. Characterization of the response behavior at the three selected elevations measured from the still water level is presented in Table 5. If one considers the

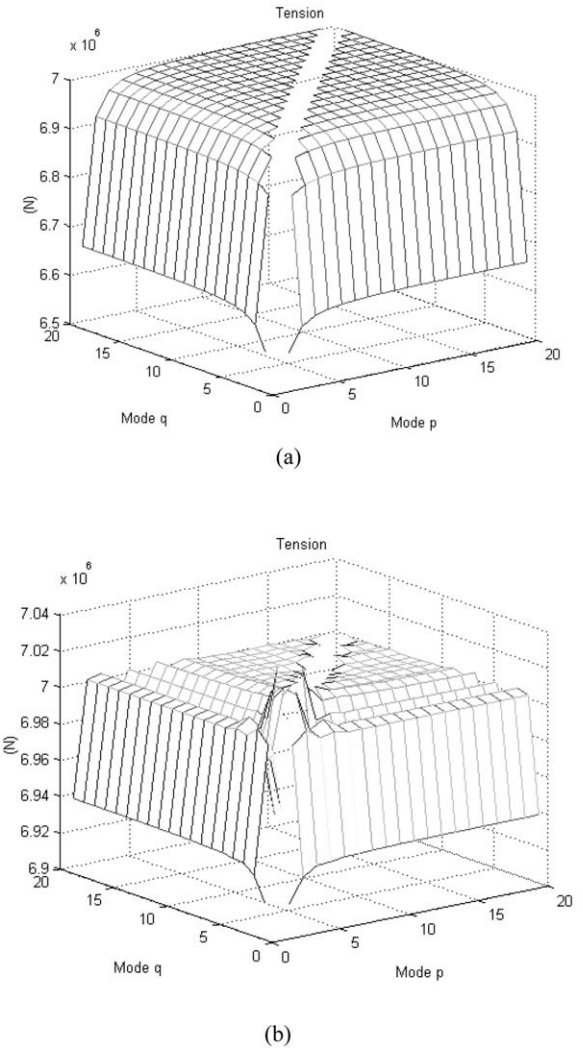

Fig. 8. Tension surface for modes p and q: (a) theoretical surface and (b) system identification estimates.

graphs of the distributions shown in Fig. 14, some interesting behavior is observed that is not obvious from the values of the skewness and kurtosis at the various water depths. In Fig. 14 a, the linear system behavior can be observed in the shape of the distribution, which appears to be Gaussian. The influence of the nonlinearities is also captured in the reduction of the peak values and broadening of the response behavior distributions. In the combined Duffing-Van der Pol model the response is dominated by the Duffing non-linearity. Since the excitation concentrated in the near surface, decaying exponentially for deep water, this combined with the fluid damping along the riser will also diminish the response behavior with depth and this should be

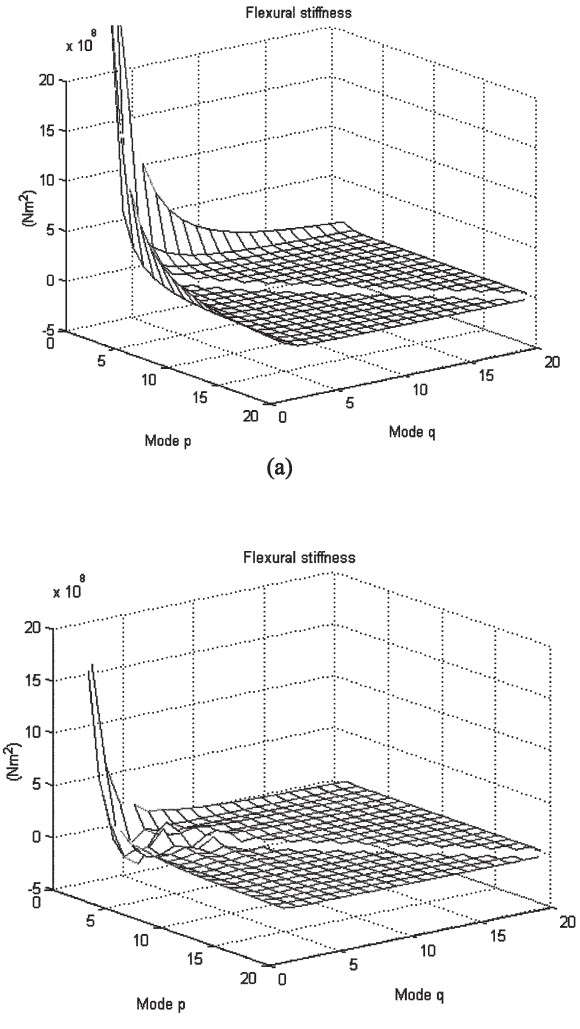

Fig. 9. Bending stiffness surface for modes p and q: (a) theoretical surface and (b) system identification estimates.

translated into reduced peaks and distribution width. This is indeed the case for the 700m-water depth, and the coalescing of the distribution width leaving only the peaks to be modified by the nonlinear models is consistent with one's intuition about the anticipated response behavior. However, at the 400 m water depth the bi-modal behavior of the distribution peaks for the Duffing and combined nonlinear models is quite interesting as is the continued domination of the response by the combined nonlinear Duffing - Van der Pol model.

Table 2
Modal values and errors of mass and viscous drag based upon using reverse system identification (0.1<f<0.4 Hz)

Modes	Mass (kg/m) Identified	Error (%)	Viscous drag (Ns/m) Identified	Error (%)
1	900.5	-1.27	116.9	-2.59
2	837.2	-8.20	113.9	-5.07
3	915.5	0.38	117.0	-2.48
4	787.6	-13.64	118.3	-1.45
5	896.1	-1.74	116.1	-3.25

Table 3
Modal values and errors of Duffing and Van der Pol coefficients based upon using reverse system identification (0.1<f<0.4 Hz)

Modes	Duffing coefficient (N/m^3) Identified	Error (%)	Van der Pol coefficient (Ns/m^3) Identified	Error (%)
1	7861.9	-1.72	4612.7	-7.75
2	8039.4	0.49	4436.6	-11.27
3	8067.6	0.84	4173.9	-16.52
4	8222.2	2.78	4588.3	-8.23
5	7944.1	-0.70	4650.4	-7.00

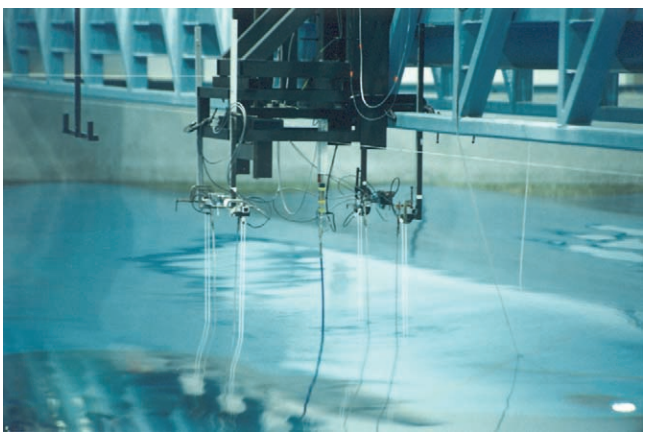

Fig. 10. Experimental setup in the model basin for riser and tendon model tests.

Table 4
Marine riser particulars for model basin tests

	Units	Model scale value	Full scale equivalent value
ABS casing outer diameter	mm	12.7	698.5
Steel core outer diameter	mm	2.5	N/A
Riser length	m	15.873	873
Dry weight	kg	2.77	46.1×10^4
Wet weight	kg	0.71	11.8×10^4
Top tension	N	41.1	68.4×10^5
Estimated bending stiffness	Nm^2	3.33	1.68×10^9

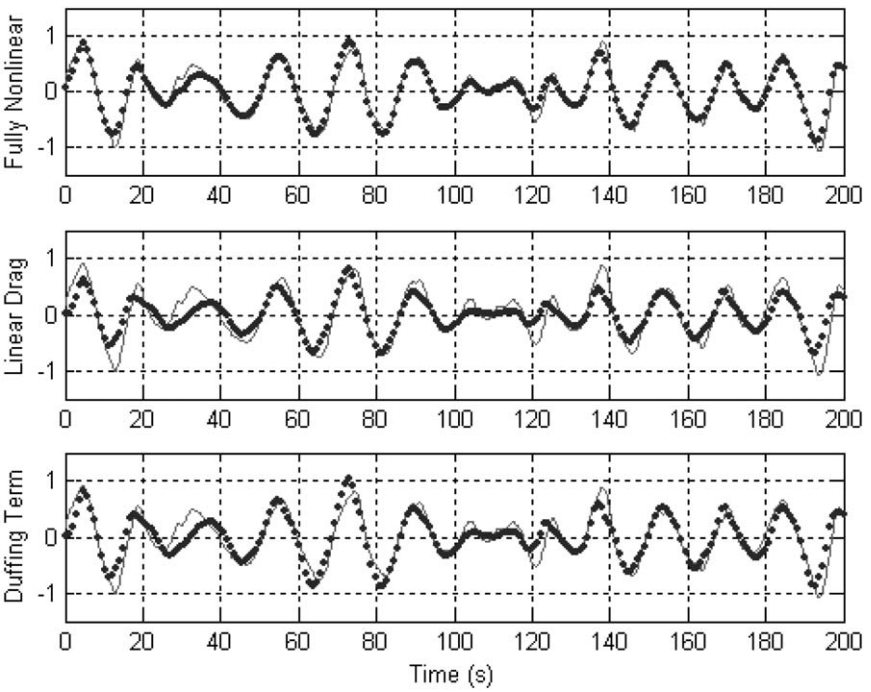

Fig. 11. Comparison of three different wave force model simulations with model test data (solid line).

5. Summary and conclusion

Reverse system identification procedures are often applied to problems that can be modeled using ordinary differential equations with constant coefficients where any non-linearity is introduced through an additional term in the equations of motion. Duffing, Van der Pol, polynomial and many other types of non-linear terms can be introduced depending upon the physical problem. The coefficients in these additional terms are also assumed to be constant. However, for many problems of interest the

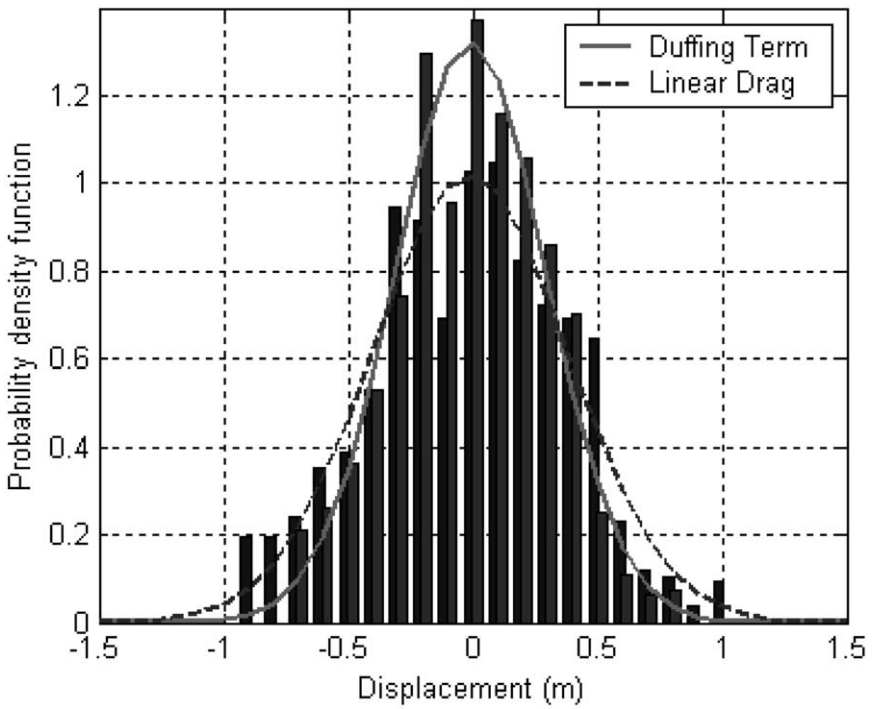

Fig. 12. Comparison of distributions for linear drag and Duffing model.

modeling of the systems require discretization and lead quite naturally to the need to address distributed-parameter systems, whose dynamic response is governed by partial differential equations, including both time and space as independent variables. Another practical consideration that will require further study is the resolution of parameters that have both constant and frequency dependent behavior. In this research study a general system identification methodology for these engineering systems was presented that involves the use of both generalized coordinate and force functions to recover the value of the generalized parameters for each mode of vibration. The introduction of analytical mode shapes resulted in a simplification of the analysis. Discrete values based upon the structural discretization do not pose a significant problem since one would merely evaluate the integrals numerically. Because of the cyclical nature of the methodology presented, the system identification procedures presented can be used to check on the accuracy of numerical simulations procedures.

To illustrate the method a single marine riser modeled as a partial differential equation was transformed into a set of ordinary differential equations using modal analysis of the forced dynamic response. The analysis method presented requires that both excitation and response of the system be known as functions of time and space. Complete data measurements of this kind are generally quite rare, so in order to test the method synthetic data sets were created. The numerical example illustrated

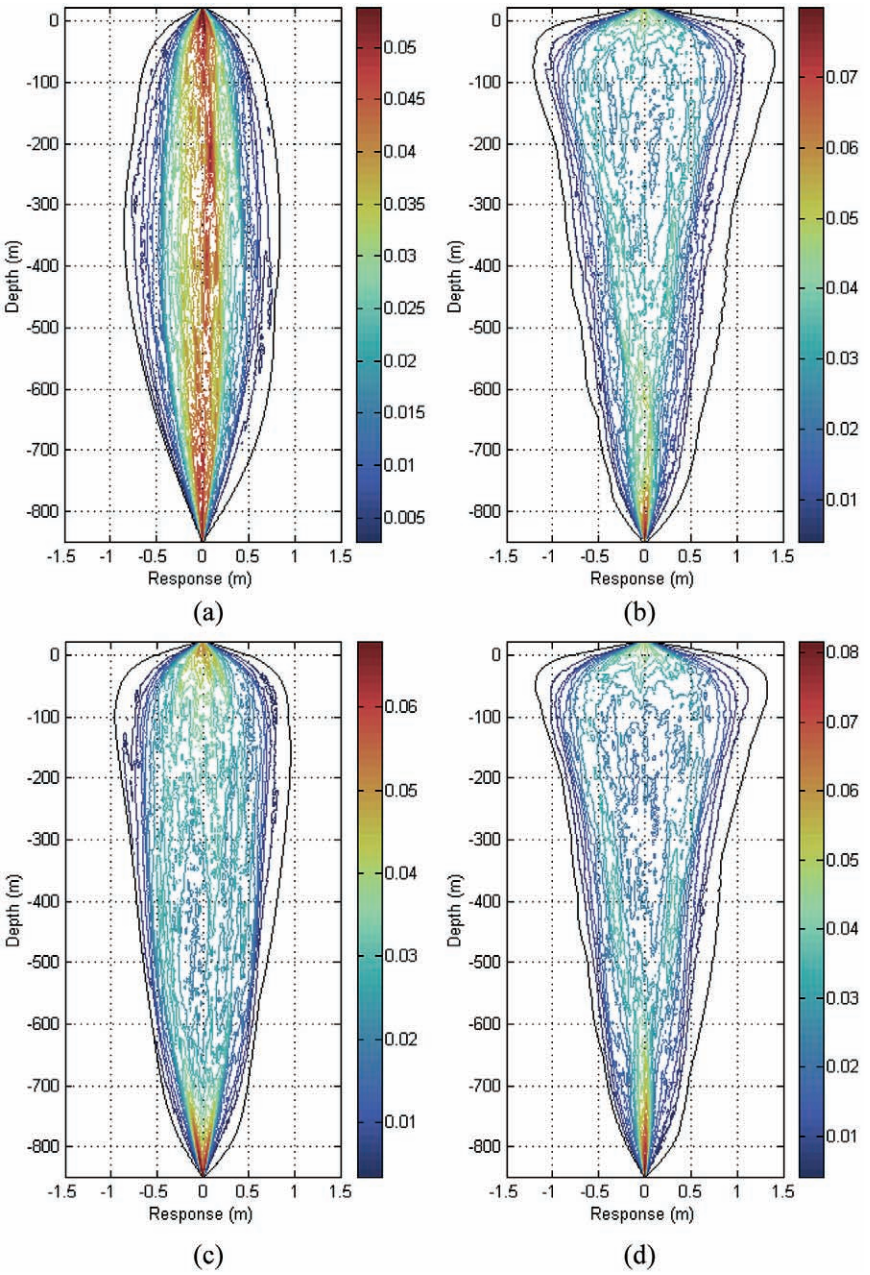

Fig. 13. Probability density functions for (a) linear drag force, (b) linear drag force with the Duffing nonlinear model included, (c) linear drag force with the Van der Pol nonlinear model included, (d) linear drag force with the Duffing and Van der Pol nonlinear models included.

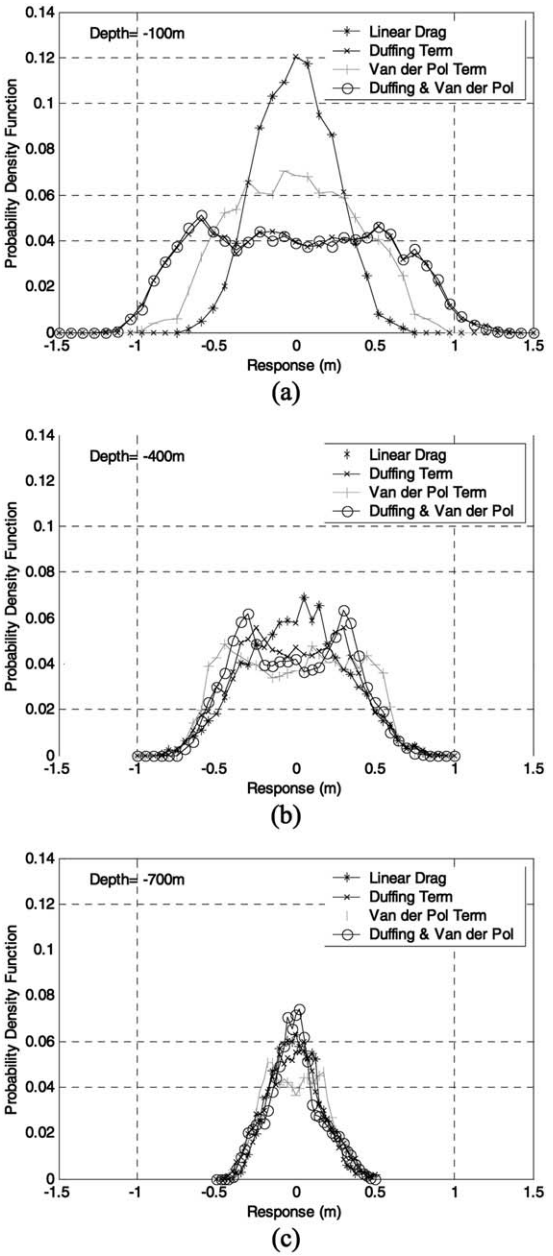

Fig. 14. Probability density function profiles at three different depths.

Table 5
Statistical characterization at selected water depths of (a) 100m, (b) 400m, and (c) 700m

(a) Depth=–100m Model	Mean	Variance	Skewness	Kurtosis
Linear Drag	–0.0014	0.0553	0.0260	2.6278
Duffing Term	–0.0063	0.2978	0.0563	1.9503
Van der Pol Term	–0.0029	0.1430	0.0435	2.2487
Duffing & Van der Pol	–0.0056	0.2961	0.0512	1.8960
(b) Depth=–400m				
Model	Mean	Variance	Skewness	Kurtosis
Linear Drag	–0.0042	0.0937	-0.0168	2.5563
Duffing Term	–0.0121	0.1095	0.0367	2.1791
Van der Pol Term	–0.0086	0.1341	0.0122	1.8295
Duffing & Van der Pol	–0.0109	0.1098	0.0266	1.8844
(c) Depth=–700m				
Model	Mean	Variance	Skewness	Kurtosis
Linear Drag	–0.0026	0.0238	0.2237	2.8137
Duffing Term	–0.0089	0.0309	0.1766	2.6949
Van der Pol Term	–0.0054	0.0341	0.1204	2.2591
Duffing & Van der Pol	–0.0083	0.0272	0.1913	2.7839

one approach to this common problem and the benefits of this approach. The white noise simulation results were presented in order to assess the accuracy of the methodology and to highlight deviations of results obtained via simulation procedures from analytical results. It was demonstrated that the accuracy of the evaluation depends upon the level of discretization employed in the numerical simulations, as well as the selection of which normal modes of vibration are used in the system identification procedure.

The study provides one with a sense of the difficulty in analyzing practical distributed-parameter systems was illustrated. There are several interesting implications for laboratory and field measurement programs of risers. In particular, using the system identification on the measured data regardless of the source will require one to choose a finite number of the most important parameters to be investigated. Assumptions regarding the wave field, the wave force excitation model and its coefficients, and the riser system are required to resolve the parameters as was demonstrated in this study. At about mid-water depth, when the excitation is provided only by surface wave phenomena, the nature of the distribution of the response may be characterized prior to numerical analysis, and this interpretation of the data may provide an indication of the nature of the non-linearity that dominates the response behavior. The determination of the magnitude of the nonlinear coefficients requires use of the procedures presented herein.

Acknowledgements

The writers gratefully acknowledge the partial financial support of the Offshore Technology Research Center and the Minerals Management Service during this study. The first writer also would like to thank the Wofford Cain foundation for their support during this study.

Appendix A: Riser model simulation using a Finite-Difference method

The governing equation for the marine riser derived in this study does not have an easily obtainable analytical solution, so solving this equation requires the use of numerical methods. In general, the method of finite difference provides a straightforward and accurate process for solving partial differential equations involving two independent variables (Smith, 1978). In the present study, spatial and temporal terms in the partial differential equations are obtained using finite difference techniques.

In order to derive the difference equation, we first introduce a finite rectangular grid on the space-time domain $W = \{(x,t):0\leq x\leq L,\ 0\leq t\leq T\}$ bounded by L, the riser length and T, the duration of the simulation. Let M and N be two positive integers and set the spatial and temporal step sizes such as

$$\Delta x = \frac{L}{M} \text{ and } \Delta t = \frac{T}{N} \tag{59}$$

Assuming that the exact solution has a bounded fourth derivative (v is C^4), we obtain the following finite forward and central difference approximations by expanding the displacement, $v(x,t)$, into a Taylor series. One then obtains

$$\left(\frac{\partial v}{\partial t}\right)_{(i,j)} = \frac{v_{i,j+1}-v_{i,j}}{\Delta t} + O(\Delta t) \tag{60}$$

$$\left(\frac{\partial^2 v}{\partial t^2}\right)_{(i,j)} = \frac{v_{i,j+1}-2v_{i,j}+v_{i,j-1}}{(\Delta t)^2} + O((\Delta t)^2) \tag{61}$$

$$\left(\frac{\partial v}{\partial x}\right)_{(i,j)} = \frac{v_{i+1,j}-v_{i,j}}{\Delta x} + O(\Delta x) \tag{62}$$

$$\left(\frac{\partial^2 v}{\partial x^2}\right)_{(i,j)} = \frac{v_{i+1,j}-2v_{i,j}+v_{i-1,j}}{(\Delta x)^2} + O((\Delta x)^2) \tag{63}$$

$$\left(\frac{\partial^4 v}{\partial x^4}\right)_{(i,j)} = \frac{v_{i+2,j}-4v_{i+1,j}+6v_{i,j}-4v_{i-1,j}+v_{i-2,j}}{(\Delta x)^4} + O((\Delta x)^4) \tag{64}$$

where, $v_{i,j} = v(i\Delta x, j\Delta t)$ and $\Delta x \to 0$, $\Delta t \to 0$.

Substituting Eq. (60) through (64) into Eq. (16) yields

$$v_{i,j+1} = \left(f_L - EI\frac{v_{i+2,j} - 4v_{i+1,j} + 6v_{i,j} - 4v_{i-1,j} + v_{i-2,j}}{(\Delta x)^4} + T_{i,j}\frac{v_{i+1,j} - 2v_{i,j} + v_{i-1,j}}{(\Delta x)^2} + w_{i,j}\frac{v_{i+1,j} - v_{i,j}}{\Delta x} \right.$$
$$\left. - M_{i,j}\frac{-2v_{i,j} + v_{i,j-1}}{(\Delta t)^2} + c_{i,j}\frac{v_{i,j}}{\Delta t} + \left(\frac{c_{3_{i,j}}}{3\Delta t} - k_{3_{i,j}}\right)v_{i,j}^3 \right) \Big/ \left(\frac{M_{i,j}}{(\Delta t)^2} + \frac{c_{i,j}}{\Delta t} + \frac{c_{3_{i,j}}}{3\Delta t}v_{i,j}^2 \right) \quad (65)$$

This implicit finite difference formula for the marine riser allows for the evaluation of the displacement at the specified node at time $t_{j+1} = (j + 1)\Delta t$, once the displacements at times t_{j-1} and t_j have been determined. The stability of this method depends on the temporal and spatial step sizes.

References

Banks, H.T., Kunisch, K., 1989. Estimation techniques for distribut parameter systems. In: Systems & Control: Foundations & Applications. Vol. 1. Birkhauser, Boston, MA.

Bendat, J.S., 1990. Nonlinear System Analysis and Identification from Random Data. John Wiley & Sons, New York, NY.

Bendat, J.S., 1993. Spectral techniques for nonlinear system analysis and identification. Shock and Vibration 1 (1), 21–31.

Bendat, J.S., 1998. Nonlinear Systems Techniques and Applications. John Wiley & Sons, New York, NY.

Bendat, J.S., Piersol, A.G., 1993. Engineering Applications of Correlation and Spectral Analysis, second ed. John Wiley & Sons, New York, NY.

Clough, R.W., Penzien, J., 1993. Dynamics of Structures, second ed. McGraw-Hill, Inc, New York, NY.

Imai, H., Yun, C.-B., Maruyama, O., Shinozuka, M., 1989. Fundamentals of system identification in structural dynamics. Probabilistic Engineering Mechanics 4 (4), 162–173.

Jones, N.P., Shi, T., Ellis, J.H., Scanlan, R.H., 1995. System identification procedure for system and input parameters in ambient vibration surveys. Journal of Wind Engineering and Industrial Aerodynamics 54/55, 91–99.

Krolikowsky, L.P., Gay, T.A., 1980. An improved linearization technique for frequency domain riser analysis. Offshore Technology Conference, OTC 3777, pp. 341–353.

McIver, D.B., Olson, R.J., 1981. Riser Effective Tension—Now You See It, Now You Don't! ASME Proceedings of the 37th Petroleum Mechanical Engineering Workshop & Conference, pp. 177–187.

Narayanan, S., Yim, S.C.S., 2000. Nonlinear model evaluation via system identification of a moored structural system. Proceedings tenth International Offshore and Polar Engineering Conference.

Panneer-Selvam, R., Bhattacharyya, S.K., 2001. Parameter identification of a compliant nonlinear sdof system in random ocean waves by reverse MISO method. Ocean Engineering 28, 1199–1223.

Rice, H.J., Fitzpatrick, J.A., 1991. A procedure for the identification of linear and nonlinear multi-degree-of-freedom systems. Journal of Sound and Vibration 149 (3), 397–411.

Rijken, O.R., 1997. Dynamic Response of Marine Risers and Tendons. Ph.D. Dissertation, Department of Civil Engineering, Texas A&M University.

Sarpkaya, T., Isaacson, M., 1981. Mechanics of Wave Forces on Offshore Structures. Van Nostrand Reinhold, New York, NY.

Smith, G.D., 1978. Numerical Solution of Partial Differential Equations: Finite Difference Method. Clarendon Press, Oxford, England.

Stansby, P.K., Worden, K., Tomlinson, G.R., Billings, S.A., 1992. Improved wave force classification using system identification. Applied Ocean Research 14, 107–118.

Wheeler, J.D., 1970. Method for calculating forces produced by irregular waves. Journal of Petroleum Technology, 359–367.